ResearchOnline@JCU



This is the author-created version of the following work:

Kumar, Avishek, Al-Jumaili, Ahmed, Prasad, Karthika, Bazaka, Kateryna, Mulvey, Peter, Warner, Jeffrey, and Jacob, Mohan (2020) *Pulse plasma deposition of Terpinen-4-ol: an insight into polymerization mechanism and enhanced antibacterial response of developed thin films.* Plasma Chemistry and Plasma Processing, 40 pp. 339-355.

Access to this file is available from:

https://researchonline.jcu.edu.au/61128/

© Springer Science+Business Media, LLC, part of Springer Nature 2019

Please refer to the original source for the final version of this work:

https://doi.org/10.1007/s11090%2D019%2D10045%2D2

Pulse Plasma Deposition of Terpinen-4-ol: An Insight into Polymerization Mechanism and Enhanced Antibacterial Response of Developed Thin Films

Avishek kumar¹, Ahmed AL-Jumaili¹, Karthika Prasad², Kateryna Bazaka^{1,2}, Peter Mulvey³, Jeffrey Warner⁴, Mohan V. Jacob^{1*}

¹Electronics Materials Lab, College of Science and Engineering, James Cook University, Townsville, Queensland 4811, Australia

²Institute for Future Environments, School of Chemistry, Physics and Mechanical Engineering, Queensland University of Technology, Brisbane, Queensland 4000, Australia

³AITHM, Immunology & Infectious Disease, Australian Institute of Tropical Health & Medicine James Cook University, Townsville, Queensland 4811, Australia

⁴Discipline of Biomedicine, College of Public Health, Medical and Veterinary Sciences James Cook University, Townsville, QLD 4811 AUSTRALIA

*Corresponding author: Mohan.Jacob@jcu.edu.au

Abstract

Antifouling/antibacterial coating derived from sustainable natural resource for biomedical devices have showed promising outcomes especially to prevent bacterial growth. Herein pulse-plasma chemical vapour deposition method is used to fabricate antimicrobial coating from Terpinen-4-ol, a tea tree oil based precursor. In this manuscript, during RF plasma polymerisation pulsed plasma is used to retain the pristine monomer structure in the developed stable coating and thereby enhanced its antibacterial activity. The developed films have tunable physical and chemical properties. Diverse film surface properties were obtained by varying the plasma deposition parameters, mainly the deposition mode (pulse and continuous wave) and duty cycle. The role of film wettability on degree of bacterial attachment has been elucidated. Overall, the number of viable bacteria on all the deposited coatings (25-30 %) were reduced to half with respect to the control (56 %).

Keywords: Pulse-PECVD; Polymer thin films; Antibacterial coatings; Plasma polymers

1. Introduction

Bacterial colonization and subsequent biofilm formation on solid surfaces pose a challenging problem to public health and negatively affect performance of many industrial processes[1, 2]. Approximately 650,000 patients are affected by hospital acquired infections (HAI) annually which costs about \$40 billion to healthcare system in US alone[3, 4]. Approximately 80 % of microbial infections are related to bacterial colonization and biofilm formation on medical implants[5, 6]. Pathogens such as *Escherichia coli* and *Pseudomonas aeruginosa* have been isolated from these infections[5, 7]. *P. aeruginosa* in particular have been found to cause a variety of biofilm mediated infections, such as tracheal stent and catheter-associated urinary tract infections [8], the bacterial infection of implantable medical devices act as reservoir of infections, impede the device correct performance and can diminish the host defense mechanism[9]. These shortcomings pose a major challenge in their future developments. Therefore, development of bioactive coatings that inhibit bacterial attachment on medical device surfaces without contributing to the development of antibiotic resistance appears as an attractive strategy to alleviate the incidence of implant-associated microbial infections.

To date, two coating strategies that notably differ in terms of their mechanism of action have been used to mitigate fouling by biological entities. Non-biocidal techniques employ surfaces that prevent the initial stages of microorganism attachment, tackling the problem at its source. PEG-based surfaces are commonly employed in this approach [10, 11], however the stability of PEG-based surfaces still remains a concern[12, 13]. The plasma deposited PEG coatings have demonstrated anti fouling properties along with a good aqueous stability[14]. Low pressure plasma enhanced chemical vapour deposition (PECVD) of PEG have extensively been carried out for development of non-fouling coatings [15-18]. Atmospheric pressure -plasma liquid deposition (PLD), PECVD and dielectric barrier discharge (DBD) techniques have used to develop PEG based non-fouling coating with robust aqueous stability[19-21]. Furthermore, specific antibodies against PEG were detected in patients during therapeutic treatment, which was not observed earlier with PEG-based drugs[22]. Biocidal coatings [23] rely on a direct interaction between microorganism and antimicrobial molecules, antibiotics or biocides incorporated in a coating [24].

Essential oils are a class of compounds which are extensively researched for their antimicrobial properties [25]. However, fabrication of solid surfaces from essential oils by conventional coating techniques like spin coating is difficult. The precise control of the molecular and macromolecular chemical structure of the polymers derived from essential oil is still a limiting factor [26]. Plasma enhanced chemical vapour deposition (PECVD) is a versatile technique for immobilization of this class of compounds on solid surfaces [27, 28]. Plasma polymerized thin films from these compounds are smooth, transparent, and have excellent chemical stability and adhesion to substrate. Their physical and chemical properties substantiate their use as protective coatings for medical devices [28-32], dielectric interlayers and encapsulating layers in electronics [33, 34]. Furthermore, tuning of plasma parameters in PECVD allows one to tailor chemical (e.g. surface energy) and physical (e.g. thickness) properties of the polymer film based on their desired applications.

Terpinen-4-ol is major bioactive component of tea tree oil. In recent decade it has enjoyed increased popularity as alternative medicine on account of its anti-microbial and antiinflammatory properties[35-38]. Terpinen-4-ol has received attention as natural antibacterial agent against bacterial species Pseudomonas aeruginosa, Escherichia coli and drug resistant *Staphylococcus aureus*[39-42] .Terpinen-4-ol penetrates through the cell wall and cytoplasmic membrane of bacteria comprimising there structure and loss of intercellular material [35, 36, 43]. Lipophilicity of the essential oils help them to penetrate through cytoplasmic membrane causing irreversible damage to cells ultimately leading to its death[44, 45]. Plasma polymers of terpinen-4-ol have a demonstrated antimicrobial behavior[28, 46]. Polymers fabricated at a low power of 10 W have been shown to be effective in reducing surface colonization and biofilm formation when tested against human pathogens *P. aeruginosa and S. aureus* [28, 46]. However, film fabricated at power of 25 W could not retain the inherent antimicrobial nature of terpinne-4-ol [35, 47, 48]. Thus, deposition power is an important parameter, which is likely to dictate the antimicrobial behavior of terpinen-4-ol plasma polymers. Higher power leads to greater fragmentation of the monomer and reduced antimicrobial behavior, whereas films deposited at power (less than 10 W) were found to be hydrolytically unstable. Previous work was focused on continuous wave plasma deposition, which leads to higher monomer fragmentation and loss of some monomer functionalities. Pulse plasma deposition partly overcomes these drawbacks of continuous wave plasma deposition.

Polymers fabricated by pulse –PECVD technique are more chemically structured and consists of more unfragmented monomer molecules. The greater retention of monomer structure in deposited film becomes of great importance in plasma deposition of bioactive monomer molecules. The duty cycle (DC) is one of the very important parameter for pulse plasma deposition and is defined as DC = ton/ toff + ton. In this work, pulsed PECVD of terpinen-4-ol thin films at a peak power of 10 W is investigated. A set of 4 duty cycles (DC-10, DC-20, DC-40, DC-100) is chosen to study the effect of the duty cycle and effective power on physical and chemical properties, namely chemical composition, surface wettability and morphology. Biological activity of the fabricated films was studied by assessing the attachment and viability of gram - negative bacteria *P. aeruginosa* on their surface. The selected species of bacteria is a strong biofilm former of clinical relevance.

2. Experimental Section

2.1 Materials

Terpinen-4-ol ($C_{10}H_{18}O$, M.W.=154.24 g/mol, Purity > 99 %, Australian Botanical Products Ltd.) was used without any further modification. Microscope cover slips (dia (Φ)=19 mm, ProSciTech, Australia) made of borosilicate glass were used as a deposition substrate. The substrates were sequentially ultrasonically (43 kHz ± 2 kHz) cleaned for 30min in baths of 5% decon 90 solution ($Decon\ laboratories\ limited$), distilled water (D.I), acetone and, finally, propanol. Fig. 1 shows the chemical scheme of Terpinen-4-ol

2.2 Sample Preparation

Pulse plasma Terpinen-4-ol (pp-Terpinen-4-ol) films were fabricated in a custom built tubular plasma reactor [49]. The separation between electrodes was kept at 8 cm for all the depositions. Clean substrates were placed in a plasma reactor and the chamber was brought to a steady pressure of 7×10^{-2} mbar. Plasma discharge was ignited using terpinen-4-ol vapors in a pulse wave mode at various duty cycles (DC) of 10, 20, 40 and 100 % at a peak power of 10 W. The pulse repetition frequency was set at 500 Hz. The T_{on} values were 0.2 ms, 0.4 ms, 0.8 ms and 2 ms for DC-10, 20, 40 and 100 respectively. The T_{off} values were 1.8 ms, 1.6 ms, 1.2ms, 0 ms for DC-10, 20, 40 and 100 respectively. The monomer was introduced into the reactor chamber after achieving a steady pressure of 7×10^{-2} mbar after plasma ignition. The monomer flow rate was kept steady at 29

cm³/min by means of a needle valve. Thin films were deposited for 15 minutes at a process pressure of 2×10^{-1} mbar for all the duty cycles.

2.3 Thin film characterization

Coating thickness was confirmed by variable angle spectroscopic ellipsometry (VASE J. A. Woollam, M2000 D, USA). Measurements were taken in a wavelength range of 200-1000 nm at three different angles of incidence (55°, 60° and 65°). The polymer film thickness and refractive index was modelled using a Cauchy function. The refractive index for the films deposited at DC-10, DC-20, DC-40, DC-100 were calculated to 1.50, 1.51, 1.53 and 1.56 respectively at the wavelength of 500 nm.

FT-IR spectroscopy was performed using a spectrum-100 spectrometer (Perkin Elmer,USA) operated in an ATR mode. Samples were deposited on KBr pellets for FT-IR charcteization. All FT-IR data were thickness normalized. Spectra were obtained at a resolution of 4 cm⁻¹ averaged over 124 scans. XPS was performed using Specs SAGE 150 (Specs, Germany) using a monochromatic Al K α source (hv=1486.6 eV). The spectra were collected using a 90° take-off angle. Casa XPS software was used for data analysis and C1s spectra were charge corrected relative to C-C at the binding energy of 285.0 eV.

The static contact angle was measured using a KSV CAM 101 optical contact angle measuring instrument. Wettability of all surfaces was measured for three different liquids, namely deionized water, ethylene glycol (Ajax chemicals, Australia) and diiodomethane (Merck Schuchardt OHG, Germany). A 3 µl drop of liquids was placed on the film surface and images were captured with an equipped camera. The contact angle was calculated using the Young-Laplace fitting [50]. The values reported here are a mean of fifteen measurements per sample type obtained from three independent samples. Surface energy was estimated following the Van Oss-Chaudhury-Good (VCG) method [51].

Roughness and topography of the film surface were examined using NT-MDT AFM instrument operated in a tapping mode. The roughness values were obtained from 3 μ m ×3 μ m AFM images and were averaged over three samples.

2.4 Antimicrobial activity

Pseudomonas aeruginosa (ATCC-589) cells were cultured overnight in Luria–Betani (L B) broth at 37 °C to reach a log phase. The culture was diluted to 5×10⁵ colony forming units

(CFU/ml) in a fresh LB medium. The biocidal response of pp-Terpinen-4-ol films and control (unmodified cover glass) was studied *in vitro*. pp-Terpinen-4-ol films were UV-sterilized by placing them at distance of 5 cm away from UV light source for duration of 20 minutes. UV-sterilized films and control samples were placed in 12-well cell cultured plates (Falcon, USA). 2ml of bacterial suspension was placed into each well. The samples were incubated at 37 °C for 24 hours after which they were rinsed with sterile deionized water to wash away any unattached bacteria. 3µl of each propidium iodide (PI) and SYTO9 (live/dead bacterial viability kit, Thermo Fisher Scientific, USA,) were added to a sterile 1 ml of deionized water for staining dead/live cells, respectively. A 200 µl aliquot of the staining solution was placed on the surface of the samples and allowed to incubate in the dark for 20 minutes. PI stains the dead bacterial cells red, whereas SYTO9 stains live cells as green. Samples were rinsed with sterile deionized water after incubation to wash away any excess stain.

The samples were visualized using an epifluorescence microscope (Axiovision, Zeiss). Images were captured at five random locations per sample. A minimum of three samples for each duty cycle were assessed. Images were processed using Image J software package (National Institutes of Health, USA). Bright field microscopic images were converted to 8 bit images. Threshold was adjusted in converted image to resemble the original image. An 'analyze particle plugin' was used to count the number of bacterial cells as dead (red) or alive (cyan). Viable bacterial adhesion assay data are analysed by one way analysis of variance (ANOVA) using origin pro software (version 9.). Tukey test were carried out to analyse the difference between groups.

3. Results and Discussion

3.1 Deposition rate

Plasma deposition conditions influence the film chemical and physical properties [52, 53]. Fig. 2 (a) shows the deposition rate of plasma polymerized terpinen-4-ol films deposited using pulse RF power at DC-10, DC-20, DC-40, DC-100 at a peak power of 10 W. The monomer flow rate and deposition pressure were kept constant during the process. Deposition rate (Rm) was calculated using the following equation 1 [54].:

$$R_{\rm m} = \frac{R_{\rm Mon} T_{\rm on} + R_{\rm Moff} T_{\rm off}}{T_{\rm tot}} = \frac{T_{\rm hickness}}{T_{\rm tot}}$$
 (1)

where R_{Mon} and R_{M off} are deposition rates during 'plasma on' and 'plasma off' periods, respectively. R_{Mon} was considered equal to R_{cw}, which is the deposition rate in a continuous wave mode (CW) at the same peak power; $R_{Mon} = R_{cw}$. The strong dependency of the film growth rate on the duty cycle suggests an occurrence of different polymerization mechanisms (e.g. plasma polymerization, chemical radical chain reaction, dissociation, etching, and ionization) during pulse PECVD of terpinen-4-ol. An increase in the deposition rate with the duty cycle indicates deposition is occurring in the power deficient region of the plasma. An increase in the deposition rate can be attributed to the increasing T_{on} with an increase in the duty cycle. At lower duty cycles (long T_{off}), there is a sharp decrease in the concentration of film-forming species (i.e. free radicals and ions), which may account for the low deposition rate. Plasma polymerization dominates the chemical radical chain reaction at a higher duty cycle (short Toff). Each molecule is fragmented to a greater degree as result of passing through a greater number of plasma discharges before arriving at the substrate. There is an increase in the polymeric chain terminations at the surface of the substrate due to high production of radicals with an increasing duty cycle. Fig. 2 b shows the deposition rate during 'plasma on' and 'plasma off' periods. R_{Moff} was calculated using equation 2.

$$R_{Moff} = \frac{R_M T_{tot} - R_{Mcw} T_{on}}{T_{off}}$$
 (2)

The graph shows the deposition rate in the 'plasma off' period is lower than that in the 'plasma on' period. The flux of energetic particles (ions or electrons) decreases during the 'plasma off' period. Also, combining of the plasma phase-formed radicals with those on the surface of the growing film leads to the chain termination during $T_{\rm off}$ period, thus lowering the deposition rate. Different polymerization mechanisms such as plasma polymerization, chemical radical chain reaction, dissociation, random cross-linking, and etching can occur during deposition. However the chemical radical chain reaction polymerization is a favoured mechanism at the lower duty cycles [53, 55]. The deposition rate at the low duty cycle (long $T_{\rm off}$) period is influenced by the concentration of the adsorbed monomer ([M]), active growing chains ([M*), and initiating species, with the

deposition rate in the 'plasma off' period estimated to be approximately 24-27 nm/min. The monomer surface concentration is directly related to its vapor phase concentration which is higher at lower duty cycles (long $T_{\rm off}$). Thus the higher concentration of absorbed monomer at lower duty cycle favors the chemical radical chain reaction. The other surface reactions such as random radical recombination's, neighboring radical recombination in growing deposit also occurs but are not predominant at low duty cycles.

3.2 Film composition

Different chemical reactions, such as free radical polymerization, random cross-linking, dissociation or etching occur during a PECVD process. The specific reaction mechanisms affects the growth rate, structure and chemical composition of the deposited films. Fig. 3 a shows the FTIR/ATR spectra of the precursor terpinen-4-ol monomer (reference spectrum) along with pp-terpinen-4-ol films deposited at various duty cycles at a peak power of 10 W. The absorbance peak for a -C-O stretching of alkyl substituted ether is observed in the 1150-1050 cm⁻¹ region in films deposited at a duty cycle of 10, 20, and 40, while it disappears in polymers deposited at a higher duty cycle of 100. This can be observed in inset of Fig. 3.a. The peaks occurring in pristine monomer at frequency range of 1150-1050 cm⁻¹ are persevered in the samples deposited at DC-10, DC-20, DC-40 (Fig. 3 a, inset) while they collapses to a single broad peak in for the samples deposited at DC-100. This indicates the incorporation of less fragmented monomer in the film at a lower duty cycle. With an increasing duty cycle, every molecule of the monomer is subjected to a greater number of plasma discharges (T_{ON}) and thus is more likely to undergo a greater degree of dissociation. This may provide an explanation for the disappearance of the -C-O stretching of alkyl substituted ether in samples deposited at DC-100.. Phenolic -C-0 stretch is observed at 1200 cm⁻¹ in the films deposited at DC-10 and DC-20. This peak vanishes for the film deposited at DC-40 and DC-100. An increase in the peak intensity corresponding to the methyl stretch [56](2871-2879 and 2961 cm⁻¹) and methylene C-H stretch (2935 cm⁻¹) is observed with an increasing duty cycle. The change in peak intensity is significant when duty cycle increases from DC-40 to DC-100 (Fig. 3 b). An increase in the peak intensity of methylene stretch bands with respect to methyl stretching bands is indicative of a more cross-linked structure of the polymers fabricated at higher duty cycles. An increase in peak intensities at 1380 and 1460 cm⁻¹ corresponds to an increase in symmetric -C-H bend in methyl and methylene group, respectively.

Formation of a more irregular cross-linked structure at higher duty cycles seems to provide a possible explanation for the drop in the intensity of this band in films deposited at DC-100. The intensity of the peak at 1705 cm^{-1} representing -C = 0 [56] stretching in carboxyl group increases with an increasing duty cycle. A broad peak at 1660 cm^{-1} corresponds to -C = C stretching, which is only observed in films deposited at DC-100 as a likely consequence of more carbon bond substitutions. The broad peak centered around 3440 cm^{-1} is indicative of the -O-H stretch.

Table 1 Wettability, surface roughness, surface O/C ratio and binding composition of pulsed plasma polymerized terpinen-4-ol thin films

Films	Roughness	WCA	O/C	% С-С /С-Н	%C-O	% C=O	% C-OR
	(r.m.s) ,nm	(deg)		C1s	C2	C3	C4
pp-DC-	0.25 ± 0.02	42.16	0.22	67.22	26.32	4.53	1.93
10		± 0.66					
pp-DC-	0.24 ± 0.015	47.91	0.19	69.17	24.61	4.36	1.86
20		± 0.31					
pp-DC-	0.25 ± 0.02	79.42	0.20	67.76	24.51	6.34	1.39
40		± 1.56					
pp-DC-	0.44 ± 0.15	67.38	0.19	54.01	25.88	19.21	0.00
100		± 3.8					
Control	0.69 ± 0.16	36.31	-	-	-	-	
(bare		± 3.09					
cover							
glass)							

Fig. 4 shows the high-resolution C1s spectra of pp-terpinen-4-ol films deposited at different duty cycles. The table 1 shows O/C ratio of films. A high O/C ratio is observed in pp-DC-10 films... The C-O functional groups occurs around 286 eV. There is not a significant variation in the –C-O component with an increasing duty cycle. The C-O bonds are more prone to rearrangement, which can in part account for this observation [57]. The C=O component occurring at 287 eV increases with an increasing duty cycle. Ester functional groups (-O-C=O) are found to occur at 289 eV in samples deposited at DC-10, DC-20 and DC-40. From the FT-IR and XPS data a possible monomer fragmentation

pathway can be inferred. Ring opening of Terpinen-4-ol molecule occurs when it is subjected to plasma conditions at DC-10, DC-20. As the energy input level is increased (DC-40, DC-100) this is followed by phenolic –C-0 bond dissociation and also a greater fragmentation of monomer.

3.3 Film wettability

The biocompatibility of a material is influenced by its wettability and surface energy. Water contact angles (WCA) of pp-terpinen-4-ol are listed in table 5.1. The influence of the duty cycle on the WCA and surface energy are shown in Fig. 5 WCA on an unmodified substrate has also been added for reference. Both contact angle and surface energy of the pp-terpinen-4-ol films were found to increase with the duty cycle except that for DC-100 films. The variation in wettability can be ascribed to changes in the chemical composition of the films. The effect of surface roughness (table 5.1), which is less than one nm for all the pp-terpinen-4-ol surfaces, on wettability would be negligible.

An increase in hydrophobicity with the duty cycle can be attributed to a higher degree of fragmentation of monomer rings, which results in a more cross-linked polymer structure as evident from the FTIR analysis. A slight decrease in the contact angle at DC-100 can be attributed to an increased concentration of hydrophilic –C=O groups. A greater degree of fragmentation and recombination of molecules at a higher duty cycle leads to the formation of more hydrophilic functionalities (-C=O in present case). This phenomenon becomes more pronounced under a deposition regime with a high level of fragmentation.[54]

3.4 Antibacterial activity

P. aeruginosa, a gram negative pathogenic bacterium, was used to evaluate the antimicrobial activity of pp-terpinen-4-ol. This strain is a potent biofilm former and is clinically relevant. Fig. 6 shows the fluorescence microscope images of attached *P. aeruginosa* cells on the surfaces of pp-terpinen-4-ol and control samples. Viable (cyan) and non-viable (red) cells are observed on surfaces of both polymer and control samples. It can be observed that there is no colony formation on the surfaces of pp-DC-10 and pp-DC-20. These films were found to be unstable in aqueous media, which can at least in part

account for the low attachment of cells on these surfaces. pp-DC-40 shows a high degree of attachment of *P. aeruginosa* cells. The number of non-viable cells was the highest on pp-DC-40 among all the samples tested. Fig. 7(a) shows the percentage of live bacterial cells attached on the surface of pp-terpinen-4-ol as a function of duty cycle. The reduction for viable bacteria on glass coverslips (used as a control) were found to be around log (0.20). A significant decrease in the number of viable bacteria, to log(0.48),log(0.90), $\log(0.65)$, $\log(0.72)$, was observed on pp-terpinen-4-ol deposited at the duty cycle of DC-100, DC-40, DC-20, and DC-10, respectively. There is no significant difference in bacterial viability on polymers deposited at DC-10 and DC-20. Polymers fabricated at DC-40 showed the lowest percentage of viable bacteria on their surface compared to the other samples and the control. Bacterial adhesion to a surface is an intricate process that depends upon the wettability, roughness, charge and chemistry of the surface, as well as properties of the microorganism [58-60]. Hydrophobic surfaces thermodynamically favourable to settlement by hydrophobic cells and likewise is observed for hydrophilic surfaces also [61, 62]. P. aeruginosa strains have been found to be relatively hydrophobic in nature [63, 64]. This explains the relatively high level of attachment of the cells to pp-terpinen-4-ol deposited at DC-40, which is relatively more hydrophobic compared to other pp-terpinen-4-ol polymers (Fig. 7b). Relatively hydrophobic surface of deposited terpinen-4-ol plasma polymer at DC-40 as compared to DC-10,DC-20 and DC-100,favors the water elimination at solid-liquid interface, facilitating close approach of bacterial cells to surface [65, 66]. Also the biocidal nature of terpinen-4-ol plasma polymers explains the huge amount of dead cells on the surface of DC-40 sample.

3.5 Stability test

The values for the static WCA and loss of thickness after an incubation in deionized water for 24 hr are shown in Fig. 8. For pp-terpinen-4-ol films, stability in water increased with the increasing duty cycle. The thickness loss of coatings deposited at DC-10 and DC-20 were around 90 % and 70 %, respectively. A relatively low degree of cross-linking and high hydrophilic character of these films make them highly dissolvable under aqueous conditions. Elution of low molecular weight chains from the films leads to a significant

decrease in the thickness of these films. Similar behavior has been previously reported for other types of plasma polymers [67].

There was a minimal increase in the WCA for films after 24 hrs of incubation for coatings deposited at DC-40 and DC-100. However, there was a significant increase in the water contact angle for films deposited at DC-20 after 24 hrs of immersion. A high rate of elution of hydrophilic moieties observed in DC-20 coatings would leave behind a carbon rich matrix, which can to some extent explain an increase in contact angle for these films. This reasoning can be extended to a WCA increase observed for coatings fabricated at DC-40 and DC-100, although the increase was minimal because of the lower rate of dissolution.

4. Conclusion

Antimicrobial terpinen-4-ol films were fabricated by the pulsed PECVD method. XPS characterization revealed an increase in the carbon content of films with an increasing duty cycle. FT-IR spectra suggested a possible polymerization mechanism, where at a lower duty cycle C-O bond dissociation is followed by radical chain reactions. Complete monomer ring fragmentation was observed at higher duty cycles. Polymer fabricated at a duty cycle of DC-40 (P_{eff} = 4W) and DC-100 were found to be more stable and robust when immersed in aqueous media. The obtained results show a clear a link between surface wettability and attachment of *P. aeruginosa*. High bacterial attachment was observed on polymers deposited at DC-40 because of relatively higher hydrophobicity of these surfaces. These polymers also showed the highest antibacterial activity among all the tested samples. The greater degree of preservation of monomer molecules at lower duty cycles enhances the antibacterial activity of these films.

Reference

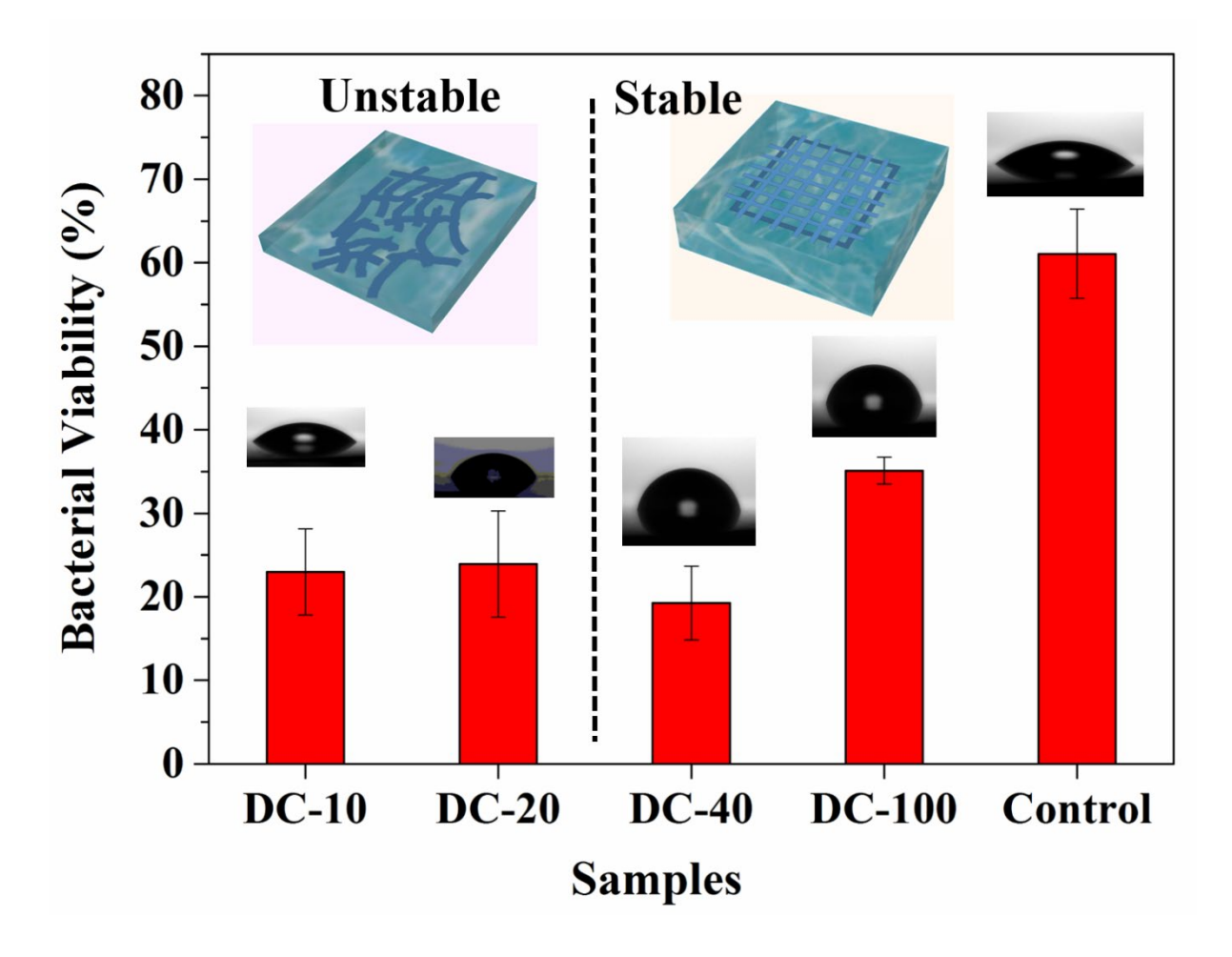
- 1. Banerjee, I., R.C. Pangule, and R.S. Kane, *Antifouling coatings: recent developments in the design of surfaces that prevent fouling by proteins, bacteria, and marine organisms.*Advanced Materials, 2011. **23**(6): p. 690-718.
- 2. Callow, J.A. and M.E. Callow, *Trends in the development of environmentally friendly fouling-resistant marine coatings.* Nature communications, 2011. **2**: p. 244.
- 3. Scott, R.D., The direct medical costs of healthcare-associated infections in US hospitals and the benefits of prevention. 2009.
- 4. Magill, S.S., et al., *Multistate point-prevalence survey of health care—associated infections.*New England Journal of Medicine, 2014. **370**(13): p. 1198-1208.
- 5. Monroe, D., *Looking for chinks in the armor of bacterial biofilms.* PLoS biology, 2007. **5**(11): p. e307.
- 6. Davies, D., *Understanding biofilm resistance to antibacterial agents.* Nature reviews Drug discovery, 2003. **2**(2): p. 114.
- 7. Nouraei, S.R., et al., *Bacterial colonization of airway stents: a promoter of granulation tissue formation following laryngotracheal reconstruction*. Archives of Otolaryngology–Head & Neck Surgery, 2006. **132**(10): p. 1086-1090.
- 8. Saini, H., et al., Azithromycin-ciprofloxacin-impregnated urinary catheters avert bacterial colonization, biofilm formation, and inflammation in a murine model of foreign-body-associated urinary tract infections caused by Pseudomonas aeruginosa. Antimicrobial agents and chemotherapy, 2017. **61**(3): p. e01906-16.
- 9. Percival, S.L., et al., *Healthcare-associated infections, medical devices and biofilms: risk, tolerance and control.* Journal of medical microbiology, 2015. **64**(4): p. 323-334.
- 10. Zanini, S., et al., *Polyethylene glycol grafting on polypropylene membranes for anti-fouling properties.* Plasma chemistry and plasma processing, 2007. **27**(4): p. 446.
- 11. Ma, H., et al., "Non-Fouling" Oligo (ethylene glycol)-Functionalized Polymer Brushes Synthesized by Surface-Initiated Atom Transfer Radical Polymerization. Advanced Materials, 2004. **16**(4): p. 338-341.
- 12. Tugulu, S. and H.-A. Klok, Stability and nonfouling properties of poly (poly (ethylene glycol) methacrylate) brushes under cell culture conditions. Biomacromolecules, 2008. **9**(3): p. 906-912.
- 13. Roosjen, A., et al., *Stability and effectiveness against bacterial adhesion of poly (ethylene oxide) coatings in biological fluids.* Journal of Biomedical Materials Research Part B: Applied Biomaterials, 2005. **73**(2): p. 347-354.
- 14. Favia, P., *Plasma deposited coatings for biomedical materials and devices: Fluorocarbon and PEO-like coatings.* Surface and Coatings Technology, 2012. **211**: p. 50-56.
- 15. Johnston, E.E., J.D. Bryers, and B.D. Ratner, *Plasma deposition and surface characterization of oligoglyme, dioxane, and crown ether nonfouling films*. Langmuir, 2005. **21**(3): p. 870-881.
- 16. Palumbo, F., et al., *RF plasma deposition of PEO-like films: diagnostics and process control.* Plasmas and polymers, 2001. **6**(3): p. 163-174.
- 17. Shen, M., et al., *Multivariate surface analysis of plasma-deposited tetraglyme for reduction of protein adsorption and monocyte adhesion.* Langmuir, 2003. **19**(5): p. 1692-1699.
- 18. Brétagnol, F., et al., Fouling and non-fouling surfaces produced by plasma polymerization of ethylene oxide monomer. Acta Biomaterialia, 2006. **2**(2): p. 165-172.
- 19. Nisol, B., et al., *Atmospheric plasma synthesized PEG coatings: non-fouling biomaterials showing protein and cell repulsion.* Surface and Coatings Technology, 2014. **252**: p. 126-133.
- 20. Nisol, B., et al., *Energetics of reactions in a dielectric barrier discharge with argon carrier gas: VI PEG-like coatings.* Plasma Processes and Polymers, 2018. **15**(3): p. 1700132.

- 21. Bhatt, S., et al., *Cell Repellent Coatings Developed by an Open Air Atmospheric Pressure Non-Equilibrium Argon Plasma Jet for Biomedical Applications*. Plasma Processes and Polymers, 2014. **11**(1): p. 24-36.
- 22. Armstrong, J.K., et al., *Antibody against poly (ethylene glycol) adversely affects PEG-asparaginase therapy in acute lymphoblastic leukemia patients*. Cancer, 2007. **110**(1): p. 103-111.
- 23. Cavallaro, A., et al., *Influence of immobilized quaternary ammonium group surface density on antimicrobial efficacy and cytotoxicity.* Biofouling, 2016. **32**(1): p. 13-24.
- 24. Tiller, J.C., et al., *Designing surfaces that kill bacteria on contact*. Proceedings of the National Academy of Sciences, 2001. **98**(11): p. 5981-5985.
- 25. Murbach Teles Andrade, B.F., et al., *Antimicrobial activity of essential oils*. Journal of Essential Oil Research, 2014. **26**(1): p. 34-40.
- 26. Wilbon, P.A., F. Chu, and C. Tang, *Progress in renewable polymers from natural terpenes, terpenoids, and rosin.* Macromolecular rapid communications, 2013. **34**(1): p. 8-37.
- 27. Bazaka, K., et al., *Anti-bacterial surfaces: natural agents, mechanisms of action, and plasma surface modification.* Rsc Advances, 2015. **5**(60): p. 48739-48759.
- 28. Bazaka, K., et al., *Plasma-assisted surface modification of organic biopolymers to prevent bacterial attachment*. Acta biomaterialia, 2011. **7**(5): p. 2015-2028.
- 29. Ershov, S., et al., *Free radical-induced grafting from plasma polymers for the synthesis of thin barrier coatings.* RSC Advances, 2015. **5**(19): p. 14256-14265.
- 30. Gulati, K., et al., *Biocompatible polymer coating of titania nanotube arrays for improved drug elution and osteoblast adhesion.* Acta biomaterialia, 2012. **8**(1): p. 449-456.
- 31. Wertheimer, M.R., *Plasma processing and polymers: a personal perspective*. Plasma Chemistry and Plasma Processing, 2014. **34**(3): p. 363-376.
- 32. Jacobs, T., et al., *Plasma surface modification of biomedical polymers: influence on cell-material interaction.* Plasma Chemistry and Plasma Processing, 2012. **32**(5): p. 1039-1073.
- 33. Ozaydin-Ince, G., A.M. Coclite, and K.K. Gleason, *CVD of polymeric thin films: applications in sensors, biotechnology, microelectronics/organic electronics, microfluidics, MEMS, composites and membranes.* Reports on Progress in Physics, 2011. **75**(1): p. 016501.
- 34. Jacob, M.V., et al., *Plasma polymerised thin films for flexible electronic applications.* Thin Solid Films, 2013. **546**: p. 167-170.
- 35. Carson, C., K. Hammer, and T. Riley, *Melaleuca alternifolia (tea tree) oil: a review of antimicrobial and other medicinal properties.* Clinical microbiology reviews, 2006. **19**(1): p. 50-62.
- 36. Greay, S.J. and K.A. Hammer, *Recent developments in the bioactivity of mono-and diterpenes: anticancer and antimicrobial activity.* Phytochemistry reviews, 2015. **14**(1): p. 1-6.
- 37. Bakkali, F., et al., *Biological effects of essential oils—a review*. Food and chemical toxicology, 2008. **46**(2): p. 446-475.
- 38. Burt, S., *Essential oils: their antibacterial properties and potential applications in foods—a review.* International journal of food microbiology, 2004. **94**(3): p. 223-253.
- 39. Halcón, L. and K. Milkus, *Staphylococcus aureus and wounds: a review of tea tree oil as a promising antimicrobial.* American Journal of Infection Control, 2004. **32**(7): p. 402-408.
- 40. Carson, C.F., B.J. Mee, and T.V. Riley, *Mechanism of action of Melaleuca alternifolia (tea tree) oil on Staphylococcus aureus determined by time-kill, lysis, leakage, and salt tolerance assays and electron microscopy.* Antimicrobial agents and chemotherapy, 2002. **46**(6): p. 1914-1920.
- 41. Hammer, K.A., C.F. Carson, and T.V. Riley, Effects of Melaleuca alternifolia (tea tree) essential oil and the major monoterpene component terpinen-4-ol on the development of single-and multistep antibiotic resistance and antimicrobial susceptibility. Antimicrobial agents and chemotherapy, 2012. **56**(2): p. 909-915.

- 42. Yang, Z., Z. Xiao, and H. Ji, *Solid inclusion complex of terpinen-4-ol/β-cyclodextrin: kinetic release, mechanism and its antibacterial activity.* Flavour and fragrance journal, 2015. **30**(2): p. 179-187.
- 43. Li, W.-R., et al., *The dynamics and mechanism of the antimicrobial activity of tea tree oil against bacteria and fungi.* Applied microbiology and biotechnology, 2016. **100**(20): p. 8865-8875.
- 44. Rasooli, I. and P. Owlia, *Chemoprevention by thyme oils of Aspergillus parasiticus growth and aflatoxin production.* Phytochemistry, 2005. **66**(24): p. 2851-2856.
- 45. Nogueira, J.H., et al., *Ageratum conyzoides essential oil as aflatoxin suppressor of Aspergillus flavus.* International Journal of Food Microbiology, 2010. **137**(1): p. 55-60.
- 46. Bazaka, K., et al., *Plasma-enhanced synthesis of bioactive polymeric coatings from monoterpene alcohols: a combined experimental and theoretical study.* Biomacromolecules, 2010. **11**(8): p. 2016-2026.
- 47. Calcabrini, A., et al., *Terpinen-4-ol, the main component of Melaleuca alternifolia (tea tree) oil inhibits the in vitro growth of human melanoma cells.* Journal of Investigative Dermatology, 2004. **122**(2): p. 349-360.
- 48. Mondello, F., et al., *In vivo activity of terpinen-4-ol, the main bioactive component of Melaleuca alternifolia Cheel (tea tree) oil against azole-susceptible and-resistant human pathogenic Candida species.* BMC infectious diseases, 2006. **6**(1): p. 1.
- 49. Jacob, M., et al., *Fabrication of a novel organic polymer thin film*. Thin Solid Films, 2008. **516**(12): p. 3884-3887.
- 50. Adamson, A.W. and A.P. Gast, *Physical chemistry of surfaces*. 1967.
- 51. Owens, D.K. and R. Wendt, *Estimation of the surface free energy of polymers*. Journal of applied polymer science, 1969. **13**(8): p. 1741-1747.
- 52. Konuma, M., *Film deposition by plasma techniques*. Vol. 10. 2012: Springer Science & Business Media.
- 53. Friedrich, J., *Mechanisms of plasma polymerization—reviewed from a chemical point of view.* Plasma Processes and Polymers, 2011. **8**(9): p. 783-802.
- 54. Zanini, S., et al., *Pulsed plasma-polymerized 2-isopropenyl-2-oxazoline coatings: Chemical characterization and reactivity studies.* Surface and Coatings Technology, 2018. **334**: p. 173-181.
- 55. Loyer, F.o., et al., Atmospheric Pressure Plasma-Initiated Chemical Vapor Deposition (AP-PiCVD) of Poly (alkyl acrylates): An Experimental Study. Macromolecules, 2017. **50**(11): p. 4351-4362.
- 56. Coates, J., *Interpretation of infrared spectra, a practical approach*. Encyclopedia of analytical chemistry, 2000.
- 57. Beamson, G., *High resolution XPS of organic polymers.* the Scienta ESCA 300 database, 1992. **208**: p. 110. 188.
- 58. Xu, L.-C. and C.A. Siedlecki, *Effects of surface wettability and contact time on protein adhesion to biomaterial surfaces.* Biomaterials, 2007. **28**(22): p. 3273-3283.
- 59. Singh, A.V., et al., *Quantitative characterization of the influence of the nanoscale morphology of nanostructured surfaces on bacterial adhesion and biofilm formation.* PloS one, 2011. **6**(9): p. e25029.
- 60. Fletcher, M. and D.C. Savage, *Bacterial adhesion: mechanisms and physiological significance*. 2013: Springer Science & Business Media.
- 61. Bos, R., H.C. Van der Mei, and H.J. Busscher, *Physico-chemistry of initial microbial adhesive interactions—its mechanisms and methods for study.* FEMS microbiology reviews, 1999. **23**(2): p. 179-230.
- 62. Bruinsma, G.M., et al., *Effects of cell surface damage on surface properties and adhesion of Pseudomonas aeruginosa.* Journal of Microbiological Methods, 2001. **45**(2): p. 95-101.

- 63. Poelstra, K., et al., *Pooled human immunoglobulins reduce adhesion of Pseudomonas aeruginosa in a parallel plate flow chamber*. Journal of biomedical materials research, 2000. **51**(2): p. 224-232.
- 64. Liu, C., et al., *Reduction of bacterial adhesion on modified DLC coatings.* Colloids and Surfaces B: Biointerfaces, 2008. **61**(2): p. 182-187.
- 65. Rodrigues, L., et al., Interference in adhesion of bacteria and yeasts isolated from explanted voice prostheses to silicone rubber by rhamnolipid biosurfactants. Journal of applied microbiology, 2006. **100**(3): p. 470-480.
- 66. Kumar, A., et al., *Biodegradable optically transparent terpinen-4-ol thin films for marine antifouling applications*. Surface and Coatings Technology, 2018. **349**: p. 426-433.
- 67. Chu, L.Q., Q. Zhang, and R. Förch, *Surface Plasmon-Based Techniques for the Analysis of Plasma Deposited Functional Films and Surfaces.* Plasma Processes and Polymers, 2015. **12**(9): p. 941-952.

Graphical Abstract



Figures

Figure 1

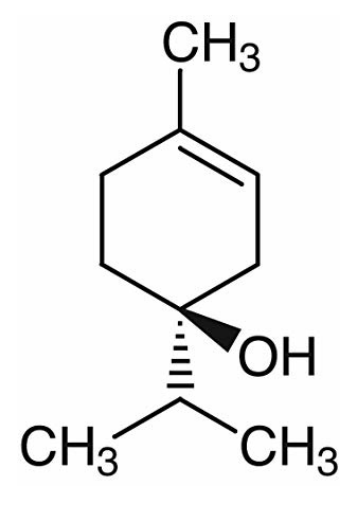


Fig. 1 Chemical scheme of terpinen-4-ol

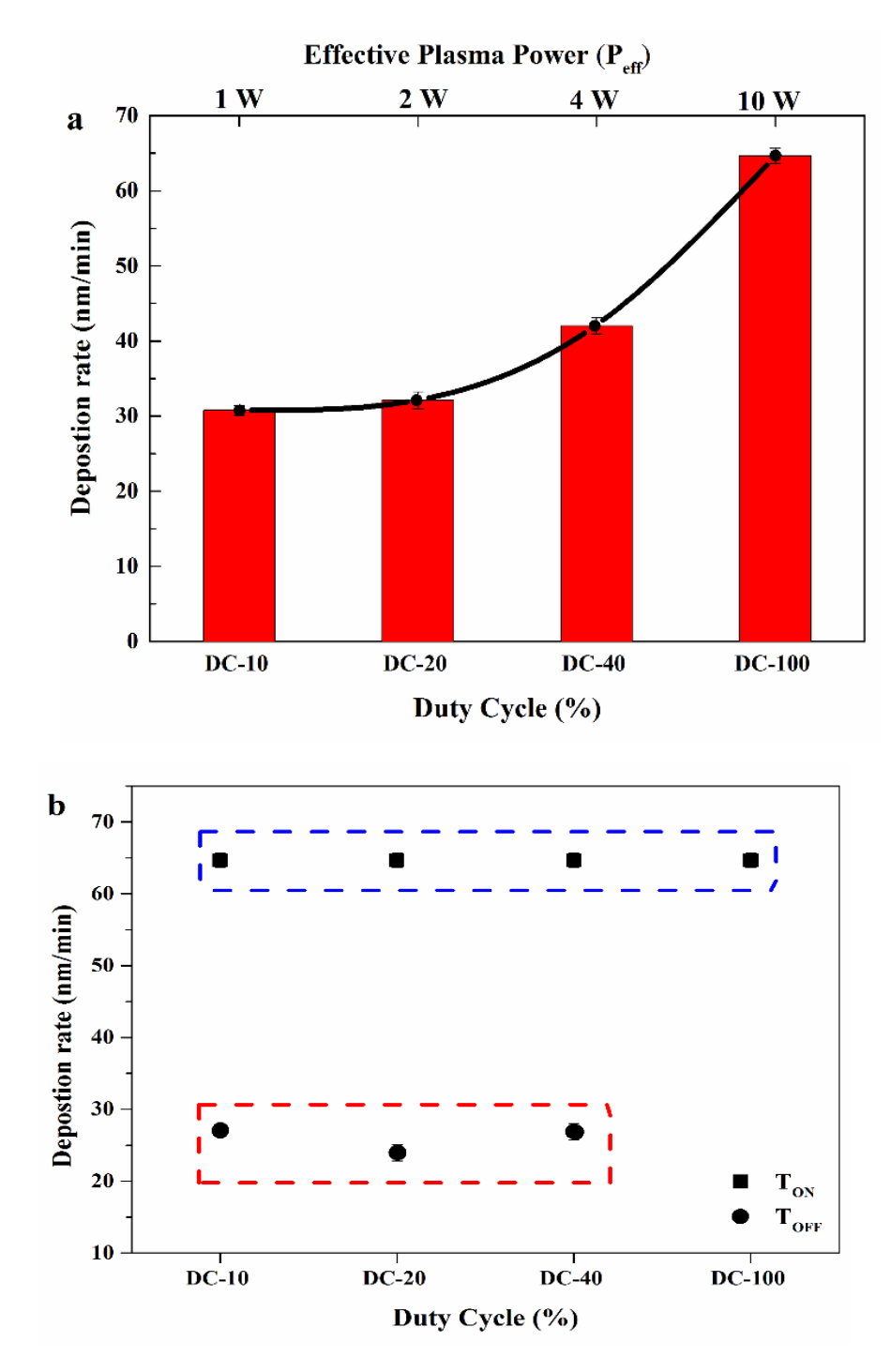


Fig. 2 (a). Deposition rate as a function of the duty cycle. (b) Influence of the duty cycle on the deposition rate during the $T_{\rm off}$ period

Figure 3

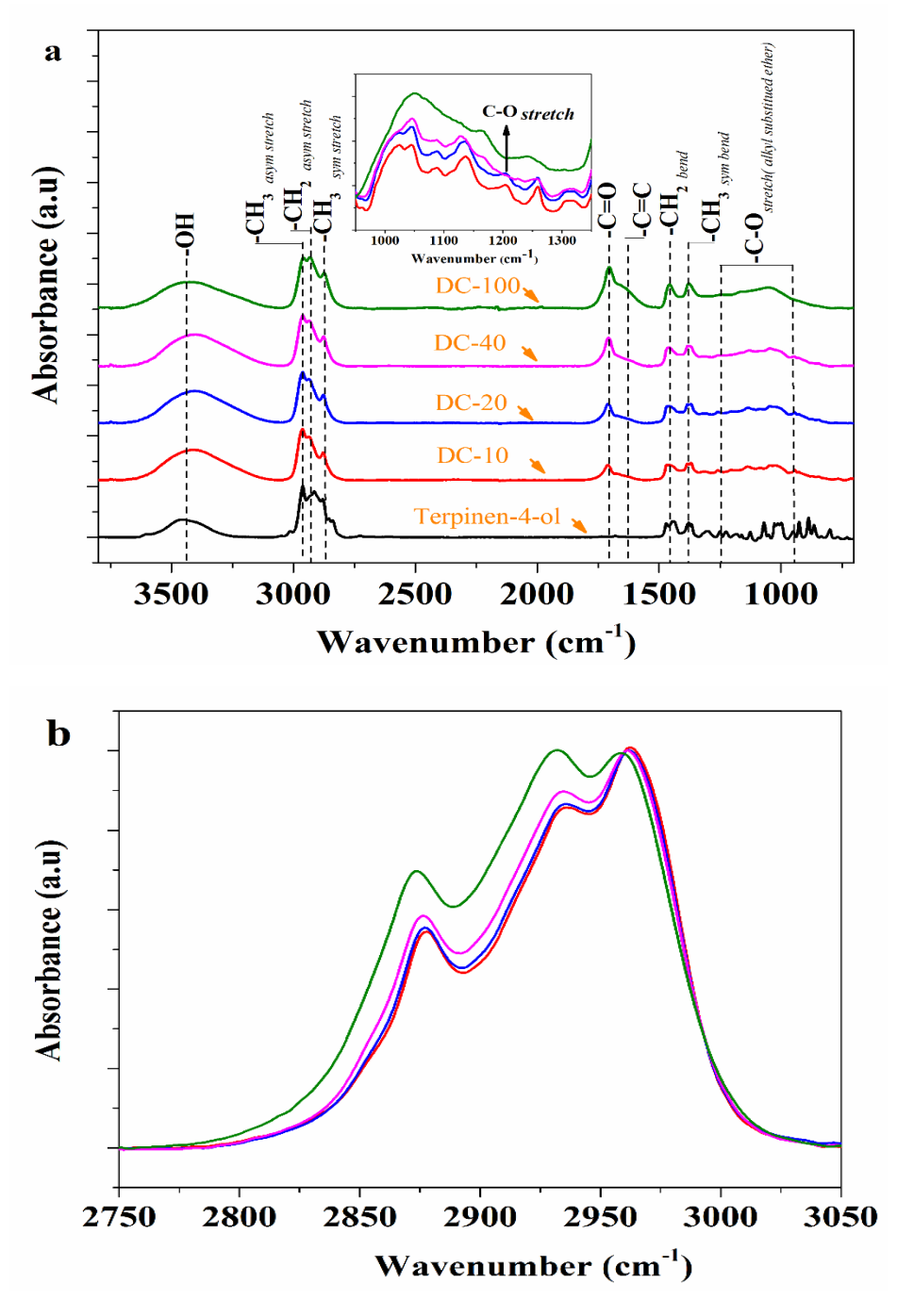


Fig. 3 (a)FT-IR spectra of pulse polymerized terpinen-4-ol thin films at different duty cycles. The spectrum for the liquid precursor has been added as a reference. (b) FT-IR spectra of films in $2700-3000 \, \text{cm}^{-1}$ range shows variation in peak intensity with increasing duty cycle

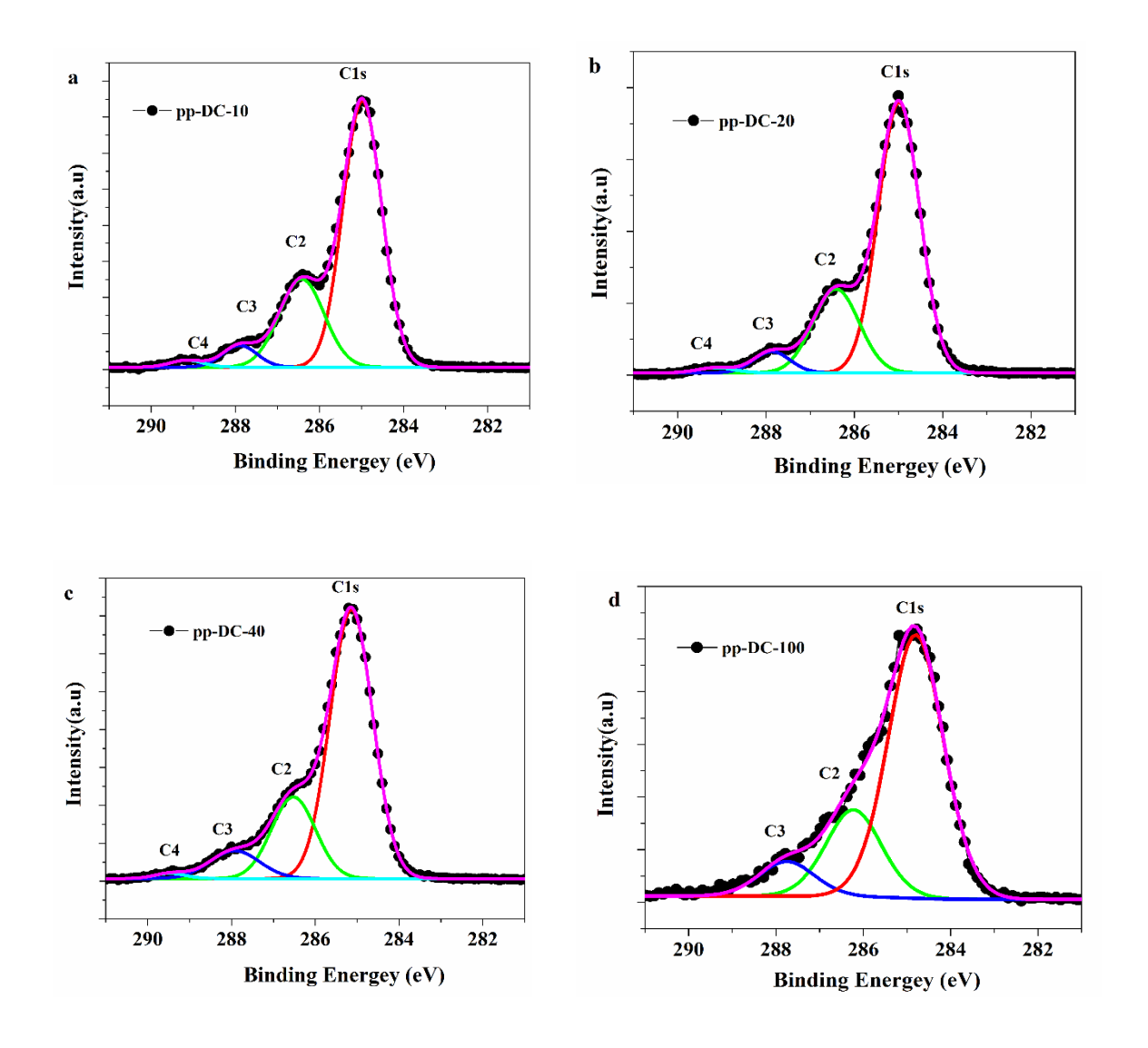
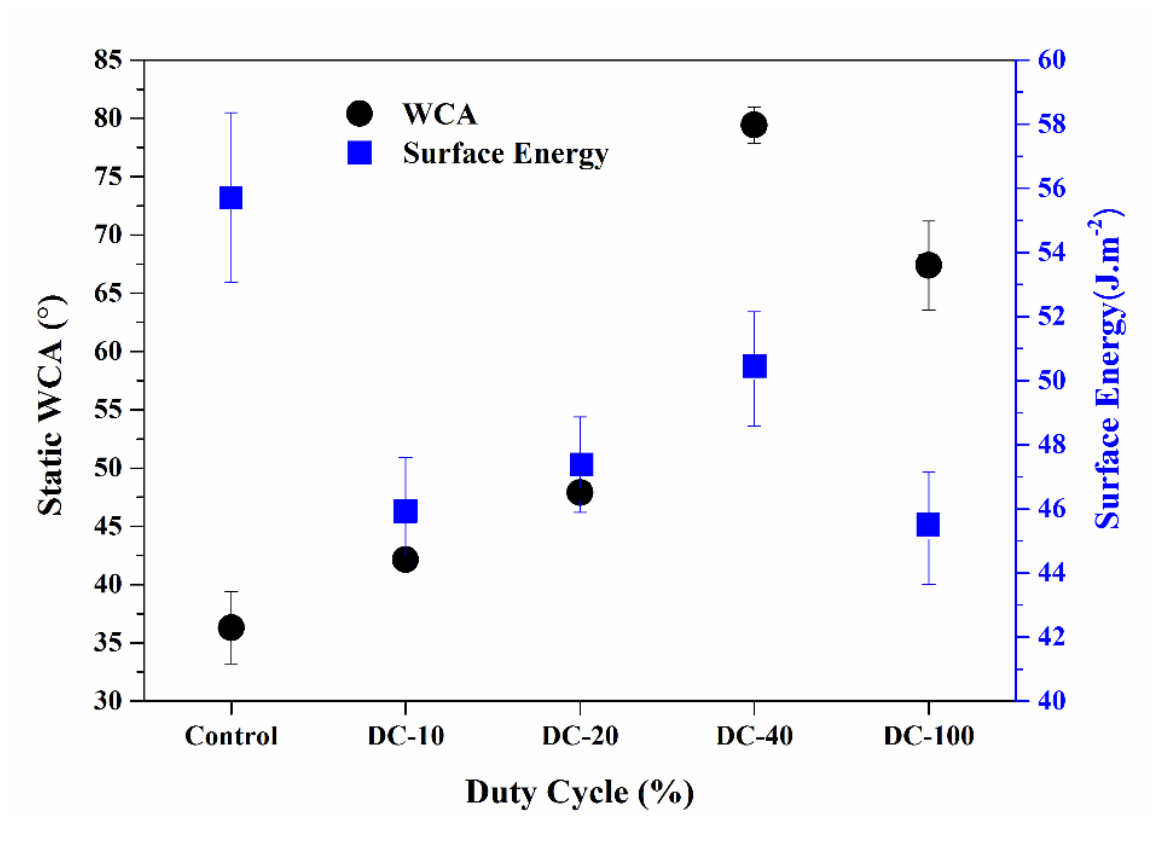


Fig. 4 High resolution C1s XPS spectra of pulse –PECVD deposited Terpinen-4-ol films at various duty cycles (a)-pp-DC-10, (b)-pp-DC-20, (c)-pp-DC-40, and (d)- pp-DC-100

Figure 5



 $\textbf{Fig. 5} \ \ \text{Static water contact angle and surface energy of films deposited at DC-10, DC-20, DC-40 and DC-100 }$

Figure 6

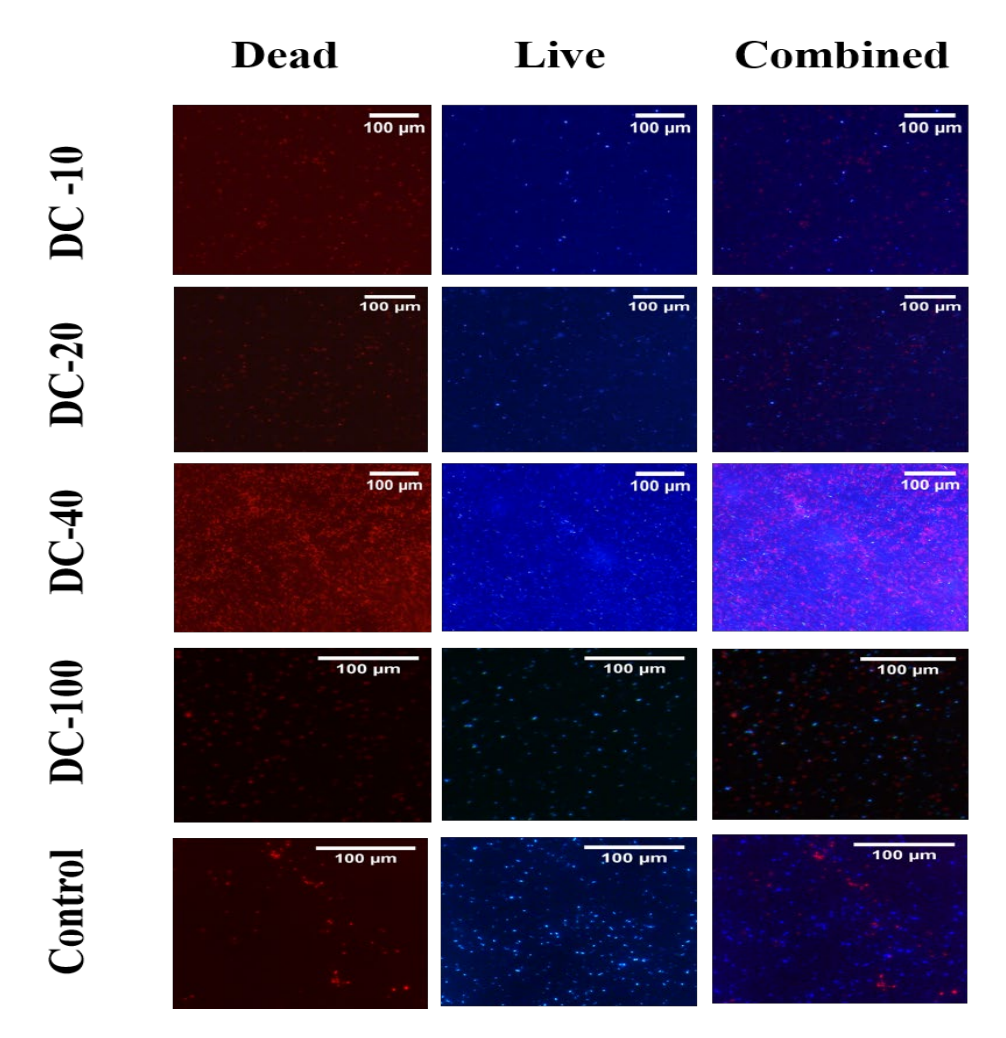
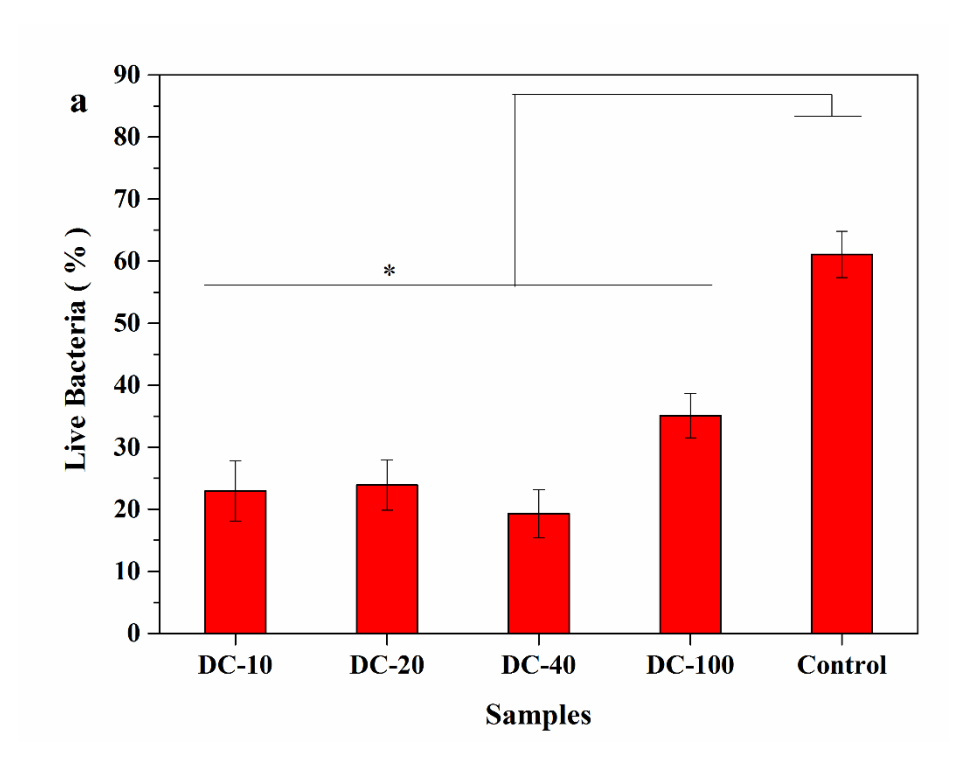


Fig. 6 Fluorescence microscopy images of *P. aeruginosa* cells attached to the surfaces of plasma polymers fabricated at different duty cycles and a control (glass slides) after 24 hr of incubation. Red is indicative of dead bacteria and cyan indicates viable cells



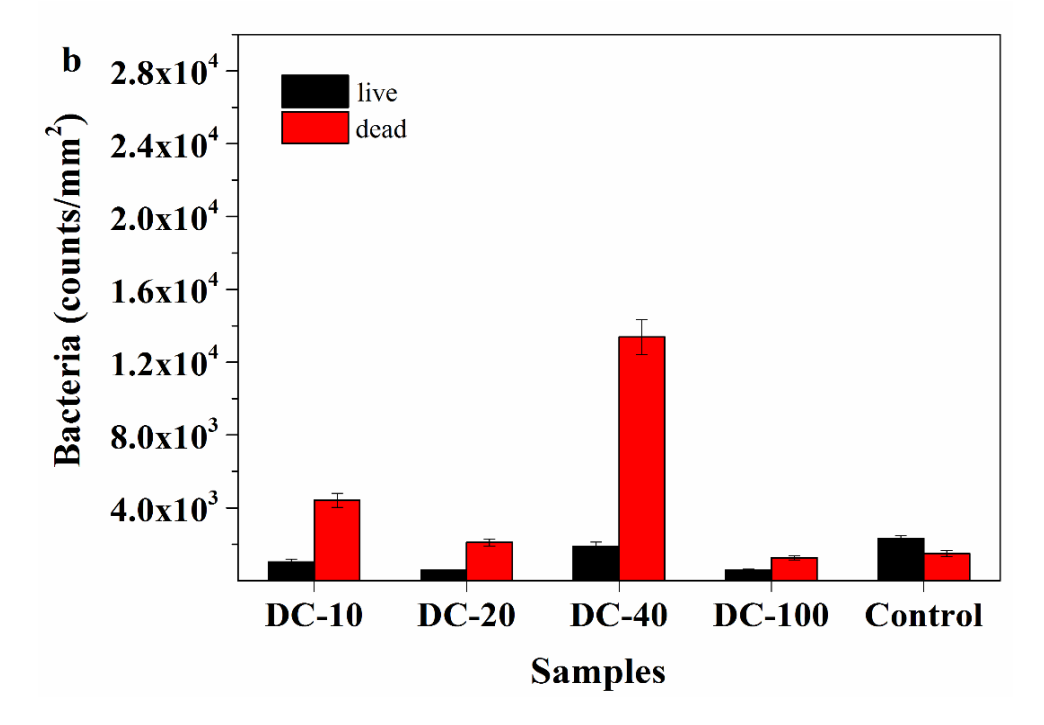


Fig. 7 (*a*) Percentage of live bacteria (* = P < 0.05). Bacterial viability between control and deposited terpinen-4-ol coatings are significantly different. (b) Total number of bacteria attached to the surface of deposited films and control after 24 hr of incubation

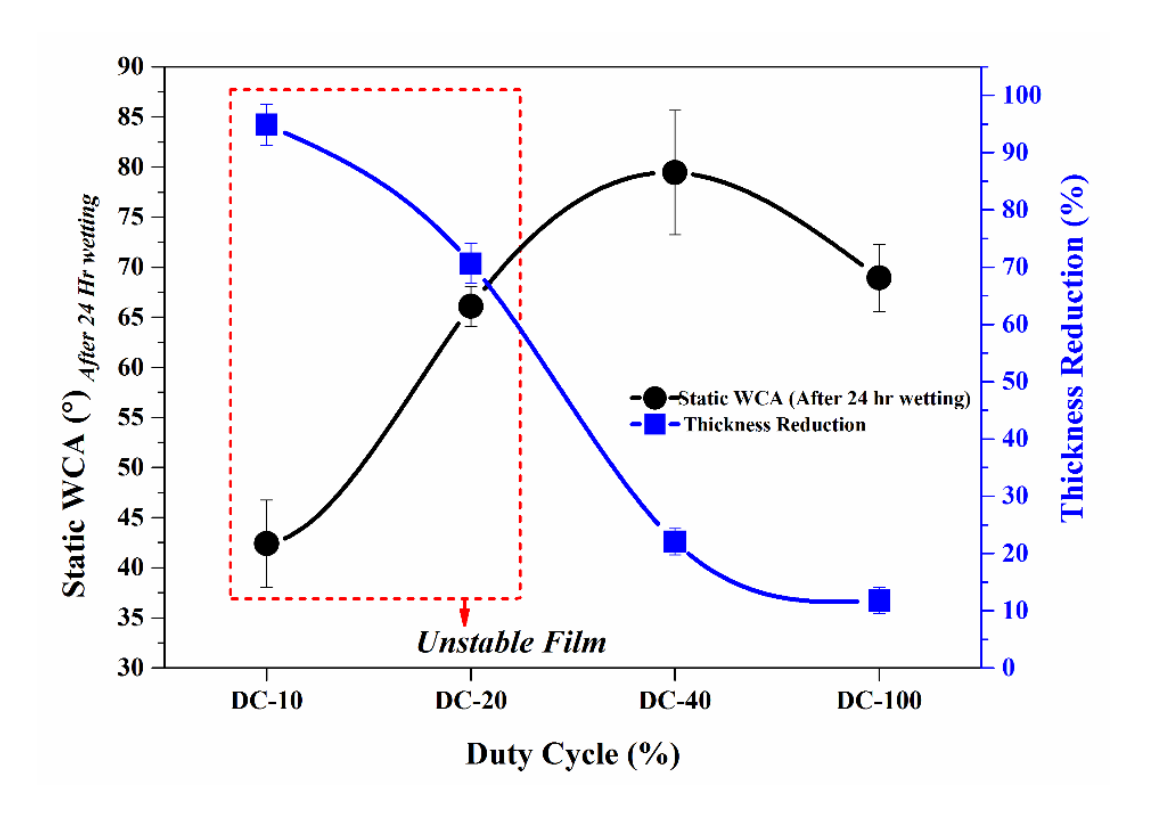


Fig. 8 Static water contact angle and percentage loss in thickness of deposited films after 24 hr immersion in aqueous media